

What do you Mean?

The Role of the Mean Function in Bayesian Optimisation

George De Ath
g.de.ath@exeter.ac.uk
Department of Computer Science
University of Exeter
Exeter, United Kingdom

Jonathan E. Fieldsend
j.e.fieldsend@exeter.ac.uk
Department of Computer Science
University of Exeter
Exeter, United Kingdom

Richard M. Everson
r.m.everson@exeter.ac.uk
Department of Computer Science
University of Exeter
Exeter, United Kingdom

ABSTRACT

Bayesian optimisation is a popular approach for optimising expensive black-box functions. The next location to be evaluated is selected via maximising an acquisition function that balances exploitation and exploration. Gaussian processes, the surrogate models of choice in Bayesian optimisation, are often used with a constant prior mean function equal to the arithmetic mean of the observed function values. We show that the rate of convergence can depend sensitively on the choice of mean function. We empirically investigate 8 mean functions (constant functions equal to the arithmetic mean, minimum, median and maximum of the observed function evaluations, linear, quadratic polynomials, random forests and RBF networks), using 10 synthetic test problems and two real-world problems, and using the Expected Improvement and Upper Confidence Bound acquisition functions.

We find that for design dimensions ≥ 5 using a constant mean function equal to the worst observed quality value is consistently the best choice on the synthetic problems considered. We argue that this worst-observed-quality function promotes exploitation leading to more rapid convergence. However, for the real-world tasks the more complex mean functions capable of modelling the fitness landscape may be effective, although there is no clearly optimum choice.

CCS CONCEPTS

• **Theory of computation** → **Gaussian processes; Mathematical optimization**; • **Computing methodologies** → **Modeling and simulation; Optimization algorithms**.

KEYWORDS

Bayesian optimisation, Surrogate modelling, Gaussian process, Mean function, acquisition function

ACM Reference Format:

George De Ath, Jonathan E. Fieldsend, and Richard M. Everson. 2020. What do you Mean? The Role of the Mean Function in Bayesian Optimisation. In *Genetic and Evolutionary Computation Conference Companion (GECCO '20 Companion)*, July 8–12, 2020, Cancun, Mexico. ACM, New York, NY, USA, 9 pages. <https://doi.org/10.1145/3377929.3398118>

GECCO '20 Companion, July 8–12, 2020, Cancun, Mexico

© 2020 Copyright held by the owner/author(s). Publication rights licensed to ACM. This is the author's version of the work. It is posted here for your personal use. Not for redistribution. The definitive Version of Record was published in *Genetic and Evolutionary Computation Conference Companion (GECCO '20 Companion)*, July 8–12, 2020, Cancun, Mexico, <https://doi.org/10.1145/3377929.3398118>.

1 INTRODUCTION

Bayesian optimisation (BO) is a popular approach for optimising expensive (in terms of time and/or money) black-box functions that have no closed-form expression or derivative information [37, 38]. It is a surrogate-based modelling approach that employs a probabilistic model built with previous function evaluations. The Gaussian process (GP) model typically used in BO provides a posterior predictive distribution that models the target function in question and quantifies the amount of predictive uncertainty. A GP is a collection of random variables, any finite number of which have a joint Gaussian distribution [34]. It can be fully specified by its mean function and kernel function (also known as a covariance function) [34]. The kernel and mean functions may be regarded as specifying a Bayesian prior on the functions from which the data are generated. The kernel function describes the structure, such as the smoothness and amplitude, of the functions that can be modelled, while the mean function specifies the prior expected value of the function at any location [37].

In BO, the location that maximises an acquisition function (or infill criterion) is chosen as the next location to be expensively evaluated. Acquisition functions combine the surrogate model's predictions and the uncertainty about its prediction to strike a balance between myopically exploiting areas of design space that are predicted to yield good-quality solutions and exploring regions that have high predicted uncertainty.

In the literature, many acquisition functions have been proposed in a number of works [12, 17, 25, 28, 39, 42], and, in general, no one strategy has been shown to be all-conquering due to the no free lunch theorem [44]. However, recent works have shown that purely exploiting the surrogate model becomes a more effective strategy as the dimensionality of the problem increases [12, 35]. Similarly, the role of the kernel function in BO has been investigated [1, 26, 29, 32, 33]. One of the most popular kernels is the radial basis function (also known as the squared exponential kernel) [38]. However, it is generally regarded as being too smooth for real-world functions [34, 40], and the Matérn family of kernels is often preferred.

Contrastingly, little attention has been paid to the role of the mean function in BO, with general practise being to use a constant value of zero [12, 17, 42], although the constant value can also be inferred from the data [37]. In general regression tasks, other mean functions have been considered, such as polynomials [5, 23, 43], and, more recently, non-parametric methods such as neural networks [13, 19]. In light of the lack of previous work into the role of the mean function in BO, we investigate the effect of different mean functions in BO in terms of both the convergence rate of the

Algorithm 1 Sequential Bayesian optimisation.

Inputs:

M : Number of initial samples
 T : Budget on the number of expensive evaluations

Steps:

```

1:  $X \leftarrow \text{SpaceFillingSampling}(\mathcal{X}, M)$             $\triangleright$  Initial samples
2: for  $t = 1 \rightarrow M$  do
3:    $f_t \leftarrow f(\mathbf{x}_t)$             $\triangleright$  Expensively evaluate all initial samples
4:  $\mathcal{D} \leftarrow \{(\mathbf{x}_t, f_t)\}_{t=1}^M$ 
5: for  $t = M + 1 \rightarrow T$  do
6:    $\theta \leftarrow \text{TrainGP}(\mathcal{D})$             $\triangleright$  Train a GP model
7:    $\mathbf{x}' \leftarrow \text{argmax}_{\mathbf{x} \in \mathcal{X}} \alpha(\mathbf{x}, \theta)$     $\triangleright$  Maximise infill criterion
8:    $f' \leftarrow f(\mathbf{x}')$             $\triangleright$  Expensively evaluate  $\mathbf{x}'$ 
9:    $\mathcal{D} \leftarrow \mathcal{D} \cup \{(\mathbf{x}', f')\}$     $\triangleright$  Augment training data
10: return  $\mathcal{D}$ 
    
```

optimisation and quality of the best found solution. Specifically, we compare the performance of using different constant values, linear and quadratic functions, as well as using random forests and radial basis function networks.

Our main contributions can be summarised as follows:

- We provide the first empirical study of the effect of using different Gaussian process mean functions in Bayesian optimisation.
- We evaluate eight mean functions on ten well-known, synthetic test problems and two real-world applications. This assessment is on a range of design dimensions (2 to 10) and for two popular acquisition functions.
- We show empirically, and explain in terms of the exploration versus exploitation trade-off, that choosing the mean function to be the constant function equal to the worst-seen so far evaluation of the objective function is consistently no worse and often superior to other choices of mean function.

We begin in Section 2 by briefly reviewing Bayesian optimisation. In Section 3 we review Gaussian processes, paying particular attention to the mean function and introduce the various mean functions we evaluate in this work. Extensive empirical experimentation is carried out on well-known test problems and a two real-world applications in Section 4. We finish with concluding remarks in Section 5.

2 BAYESIAN OPTIMISATION

Bayesian optimisation (BO), also known as Efficient Global Optimisation (EGO), is a surrogate-assisted global search strategy that sequentially samples design space at likely locations of the global optimum, taking into account both the surrogate model’s prediction $\mu(\mathbf{x})$ and the associated prediction uncertainty $\sigma(\mathbf{x})$ [22]. See [7, 14, 37] for comprehensive reviews of BO. Without loss of generality, we can define the problem of finding a global minimum of an unknown objective function $f : \mathbb{R}^d \mapsto \mathbb{R}$ as

$$\min_{\mathbf{x} \in \mathcal{X}} f(\mathbf{x}), \quad (1)$$

where $\mathcal{X} \subset \mathbb{R}^d$ is the feasible design space of interest. We assume that f is a black-box function, i.e. it has no simple closed form, but that we can have access the results of its evaluations $f(\mathbf{x})$ at

any location $\mathbf{x} \in \mathcal{X}$, although evaluating $f(\mathbf{x})$ is expensive so that the number of evaluations required to locate the global optimum should be minimised.

Algorithm 1 outlines the BO procedure. It starts (line 1) with a space filling design, typically Latin hypercube sampling [27], of the feasible space. These samples $X = \{\mathbf{x}_t\}_{t=1}^M$ are then expensively evaluated with the function $f_t = f(\mathbf{x}_t)$, and a training dataset \mathcal{D} is constructed (line 4). Then, at each iteration of the sequential algorithm, a regression model, usually a Gaussian process (\mathcal{GP}), is constructed and trained (line 6) using the current training data. The choice of where next to expensively evaluate is determined by maximising an acquisition function (or infill criterion) $\alpha(\mathbf{x})$ which balances the exploitation of regions of design space that are predicted to yield good-quality solutions and exploration of regions of space where the predictive uncertainty is high. The design \mathbf{x}' maximising $\alpha(\mathbf{x})$ is expensively evaluated and the training data is subsequently augmented (lines 7 to 9). This process is then repeated until the budget has been expended.

Two of the most popular acquisition functions are Expected Improvement (EI) [28] and Upper Confidence Bound (UCB) [39]. EI measures the positive predicted improvement over the best solution evaluated thus far, f^* :

$$\alpha_{EI}(\mathbf{x}) = \sigma(\mathbf{x}) (s\Phi(s) + \phi(s)), \quad (2)$$

where $s = (f^* - \mu(\mathbf{x}))/\sigma(\mathbf{x})$ is the predicted improvement at \mathbf{x} normalised by the uncertainty, and $\Phi(\cdot)$ and $\phi(\cdot)$ are the Gaussian cumulative density and probability density functions respectively. UCB is a weighted sum of the mean prediction and its associated uncertainty:

$$\alpha_{UCB}(\mathbf{x}) = - \left(\mu(\mathbf{x}) - \sqrt{\beta_t} \sigma(\mathbf{x}) \right), \quad (3)$$

where $\beta_t \geq 0$ is a weight that depends on the number of function evaluations t and explicitly controls the exploitation vs. exploitation trade-off. Note that both EI and UCB are presented here in the form used for minimisation. While other acquisition functions have been proposed, such as probability of improvement [25] and entropy-based methods such as predictive entropy search [17] and max-value entropy search [42], we limit our investigation to the commonly used EI and UCB to allow the focus on the mean functions themselves.

3 GAUSSIAN PROCESSES

Gaussian processes are a common choice of surrogate model due to their strengths in uncertainty quantification and function approximation [34, 37]. A GP is a collection of random variables, and any finite number of these have a joint Gaussian distribution [34]. We can define a Gaussian process prior over f to be $\mathcal{GP}(m(\mathbf{x}), \kappa(\mathbf{x}, \mathbf{x}' | \theta))$, where $m(\cdot)$ is the mean function and $\kappa(\cdot, \cdot | \theta)$ is the kernel function (covariance function) with hyperparameters θ . Given data consisting of f evaluated at t sampled locations $\mathcal{D} = \{(\mathbf{x}_n, f_n \triangleq f(\mathbf{x}_n))\}_{n=1}^t$, the posterior distribution of f at a given location \mathbf{x} is Gaussian:

$$p(f | \mathbf{x}, \mathcal{D}, \theta) = \mathcal{N}(f | \mu(\mathbf{x}), \sigma^2(\mathbf{x})) \quad (4)$$

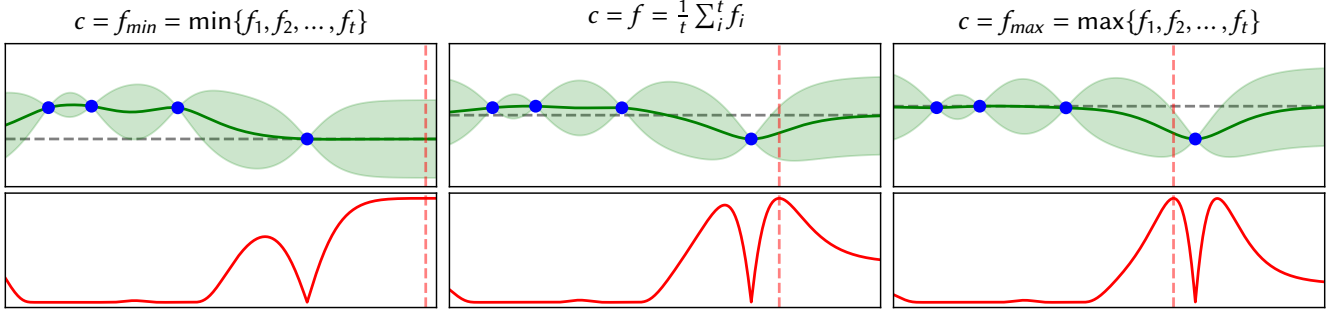


Figure 1: GP models with identical training data (blue) and kernel hyperparameters, along with different constant mean functions. The mean function used in each GP is shown (grey, dashed) and corresponds to the value of the smallest (left), arithmetic mean (centre), and largest (right) seen function values. The lower row shows the corresponding EI and its maximiser (red dashed). Note how the min and max models lead EI to prefer exploring and exploiting respectively.

with posterior mean and variance

$$\mu(\mathbf{x} | \mathcal{D}, \theta) = m(\mathbf{x}) + \kappa(\mathbf{x}, X)K^{-1}(\mathbf{f} - \mathbf{m}) \quad (5)$$

$$\sigma^2(\mathbf{x} | \mathcal{D}, \theta) = \kappa(\mathbf{x}, \mathbf{x}) - \kappa(\mathbf{x}, X)^\top K^{-1} \kappa(X, \mathbf{x}). \quad (6)$$

Here $X \in \mathbb{R}^{t \times d}$ is the matrix of design locations, $\mathbf{f} = \{f_1, f_2, \dots, f_t\}$ is the corresponding vector of true function evaluations and $\mathbf{m} = \{m(\mathbf{x}_1), m(\mathbf{x}_1), \dots, m(\mathbf{x}_t)\}$ is the vector comprised of the mean function at the design locations. The kernel matrix $K \in \mathbb{R}^{t \times t}$ is given by $K_{ij} = \kappa(\mathbf{x}_i, \mathbf{x}_j | \theta)$ and $\kappa(\mathbf{x}, X)$ is given by $[\kappa(\mathbf{x}, X)]_i = \kappa(\mathbf{x}, \mathbf{x}_i | \theta)$. In this work we use an isotropic Mat rn 5/2 kernel:

$$\kappa(\mathbf{x}, \mathbf{x}' | \theta) = \theta_0 \left(1 + \sqrt{5}r + \frac{5}{3}r^2 \right) \exp(-\sqrt{5}r), \quad (7)$$

where $r = \theta_1 \|\mathbf{x} - \mathbf{x}'\|$ and $\theta = [\theta_0, \theta_1]$, as recommended for modelling realistic functions [38]. The kernel’s hyperparameters θ are learnt via maximising the log marginal likelihood (up to a constant):

$$\log p(\mathbf{f} | X, \theta) = -\frac{1}{2} \log |K| - \frac{1}{2} (\mathbf{f} - \mathbf{m})^\top K^{-1} (\mathbf{f} - \mathbf{m}) \quad (8)$$

using a multi-restart strategy [37] with L-BFGS-B [8]. Henceforth, we drop the explicit dependencies on the data \mathcal{D} and the kernel hyperparameters θ for notational simplicity.

3.1 Mean Functions

It is well-known that the posterior prediction (4) of the GP reverts to the prior as the distance of \mathbf{x} from the observed data increases, i.e. as $\min_{\mathbf{x}_i \in \mathcal{D}} \|\mathbf{x} - \mathbf{x}_i\| \rightarrow \infty$. In particular, the posterior mean reverts to the prior mean, i.e. $\mu(\mathbf{x}) \approx m(\mathbf{x})$; and the posterior variance approaches the prior variance, θ_0 for the Mat rn kernel. The upper row of Figure 1 illustrates this effect for three different constant mean values: the best, average (arithmetic mean), and worst function values observed thus far. Note how the predicted values of the GP tend to the mean function (dashed) as the distance from the nearest evaluated location (blue) increases. The figure also shows another important, and often overlooked, aspect of the mean function: its effect on the acquisition function (lower). In this case three different locations maximise EI for the three mean functions, and it is not known *a priori* which location is preferable.

Practitioners of BO usually standardise the observations f_i before fitting the GP at each iteration, i.e. they subtract the mean of the observations and divide by the standard deviation of the relevant feature/variable after which the mean function is taken as the constant function equal to zero; that is, the effective mean function is the constant function equal to the arithmetic mean of the observed function values. In addition, the prior variance of the GP is matched to the observed variance of the function values. Although the standardisation is not usually discussed in the literature, it is commonplace in standard BO libraries, e.g. GPpyOpt [2], BoTorch [3] and Spearmint¹. It is, however, unclear whether this is the best choice for BO or whether a different mean function may be preferable. We now introduce the mean functions that will be evaluated in this work.

Here, we consider the mean function to be a set of basis functions $\mathbf{h}(\mathbf{x})$ with corresponding weights \mathbf{w} [34]:

$$m(\mathbf{x}) = \mathbf{h}(\mathbf{x})^\top \mathbf{w}. \quad (9)$$

A constant mean function with value c , for example, can be written as $\mathbf{h}(\mathbf{x}) = c\mathbf{1}$ with $\mathbf{w} = 1$. In addition to the standard constant function equal to the arithmetic mean of the data $c = \bar{f} = t^{-1} \sum_i^t f_i$, we consider three other constant values: using the best and worst seen observation’s value at each iteration, i.e. $c = f_{min} = f^* = \min\{f_1, f_2, \dots, f_t\}$ and $c = f_{max} = \max\{f_1, f_2, \dots, f_t\}$, and the median observed value $c = f_{med} = \text{median}\{f_1, f_2, \dots, f_t\}$. In comparison to using the data mean $c = \bar{f}$, using $c = f_{min}$ leads to acquisition functions becoming more exploratory, as illustrated in Figure 1 (left panel). This is because locations far away from previously evaluated solutions \mathcal{D} will have predicted means $\mu(\mathbf{x})$ equal to the f^* and with large predicted uncertainty, leading to large values of, for example, EI and UCB. Conversely, using $c = f_{max}$ will, as illustrated in Figure 1 (right panel), lead to increased exploitation due to regions far from \mathcal{D} having large uncertainty, but poor predicted values and hence small $\alpha(\mathbf{x})$. Interestingly, the effect of using $c = \bar{f}$ or $c = f_{med}$ will change over the course of the optimisation. When there are relatively few function evaluations \mathbf{f} and f_{med} will be approximately $(f_{min} + f_{max})/2$. However, as the number of

¹<https://github.com/HIPS/Spearmint>

expensive function evaluations increases and the optimisation converges towards the (estimated) optimum, \hat{f} and particularly f_{med} will tend to approach f_{min} , thus leading to increased exploration.

We also consider linear and quadratic mean functions. Linear mean functions are defined as $\mathbf{h}(\mathbf{x}) = [1, x^{(1)}, x^{(2)}, \dots, x^{(d)}]$, with corresponding weights $\mathbf{w} \in \mathbb{R}^{d+1}$ and where $x^{(i)}$ refers to the i th element of \mathbf{x} . Quadratic mean functions are defined similarly, with polynomial terms up to degree 2 and with weights $\mathbf{w} \in \mathbb{R}^q$, where $q = \binom{d+2}{d}$. To avoid overfitting to the data, these regressions are typically trained via a regularised least-squares approximation, i.e. ridge regression (also known as Tikhonov regularization). The optimal regularised weights \mathbf{w}^* are estimated by solving

$$\mathbf{w}^* = \underset{\mathbf{w}}{\operatorname{argmin}} \|\mathbf{f} - H\mathbf{w}\|^2 + \lambda \|\mathbf{w}\|^2, \quad (10)$$

where $H = [\mathbf{h}(\mathbf{x}_1), \mathbf{h}(\mathbf{x}_2), \dots, \mathbf{h}(\mathbf{x}_t)]$ and $\lambda \geq 0$ controls the amount of regularisation. The ordinary least squares estimator is

$$\mathbf{w}^* = (H^\top H + \lambda \mathbf{I})^{-1} H^\top \mathbf{f}, \quad (11)$$

In this work, the regularisation parameter λ was chosen via five-fold cross-validation for $\lambda \in \{10^{-6}, 10^{-5}, \dots, 10^1, 10^2\}$.

Another choice of basis functions are radial basis functions (RBFs), which have the property that each basis function only depends on the Euclidean distance from a fixed centre [4]. These are known as RBF networks and can be thought of as either linear neural networks using RBF activation functions [31] or as finite-dimensional Gaussian processes [4]. A commonly used set of basis functions, and the ones used in this work, are the Gaussian RBFs $\phi_i(\mathbf{x}) = \exp(-\gamma \|\mathbf{x} - \mathbf{z}_i\|)$. While any set of locations can be used as the centres \mathbf{z}_i , we place a Gaussian RBF at each of the previously-evaluated locations, i.e. $\mathbf{z}_i \equiv \mathbf{x}_i \forall i = 1, \dots, t$, resulting in $\mathbf{h}(\mathbf{x}) = [\phi_1(\mathbf{x}), \phi_2(\mathbf{x}), \dots, \phi_t(\mathbf{x})]$. Similarly to the linear and quadratic mean functions, the regularisation parameter λ and length scale γ were chosen via five-fold cross validation. Values of λ were selected in the same range as for the linear and quadratic mean functions, and the values of γ were selected from $\gamma \in \{10^{-3}, 10^{-2.5}, \dots, 10^{1.5}, 10^2\}$. A more fine-grained selection of values were chosen following a preliminary investigation which revealed the modelling error to be more sensitive to changes in γ than λ . We note here that the use of regularisation is particularly important when placing an RBF on each evaluated location because the RBF network will otherwise be able to perfectly interpolate the data. This would lead to $\mathbf{f} \equiv \mathbf{m}$ and therefore (8) would reduce to $-\frac{1}{2} \log|K|$, which can be maximised by either $\theta_0 \rightarrow 0$ or $\theta_1 \rightarrow \infty$ in (7). This results in the posterior variance estimates $\sigma^2(\mathbf{x})$ being over-confident and thus having small variance everywhere with predictions determined by the mean function.

Lastly, we include a non-parametric regressor, extremely randomised trees, better known as Extra-Trees (ET, [15]), a variant of Random Forests (RF, [6]). RFs are ensembles of classification or regression trees that are each trained on a different randomly chosen subsets of the data. Unlike RFs, that attempt to split the data at each cut-point of a tree optimally, the ET method instead selects the cut-point as the best from a small set of randomly chosen cut-points; this additional randomisation results in a smoother regression in comparison to RFs. Given that ETs use randomised

cut-points, they typically use all the training data in each tree. However, to counteract the overfitting that this will produce, we allow each item in the training set to be resampled, instead of using all elements of the set for each tree. Note that, while not presented as such here, RFs can also be interpreted as a kernel method [10, 36].

4 EXPERIMENTAL EVALUATION

We now investigate the performance of the mean functions discussed in Section 3.1 using the EI and UCB acquisition functions (Section 2) on ten well-known benchmark functions with a range dimensionality and landscape properties, and two real-world applications. Full results of all experimental evaluations are available in the supplementary material. The mean functions to be evaluated are the constant functions, $c = \hat{f}$, $c = f_{med}$, $c = f_{min}$, and $c = f_{max}$, labelled *Arithmetic*, *Median*, *Min*, and *Max* respectively, as well as the *Linear*, *Quadratic*, Extra-Trees (*RandomForest*), and RBF network-based (*RBF*) mean functions.

A Gaussian process surrogate model with an isotropic Mat rn 5/2 kernel (7) was used in all experiments. The Bayesian optimisation runs themselves were carried out as in Algorithm 1, with the additional step of fitting a mean function before training the GP (Algorithm 1, line 6) at each iteration. All test problems evaluated in this work were scaled to $[0, 1]^d$, and observations were standardised at each BO iteration, prior to mean function fitting. The models were initially trained on $M = 2d$ observations generated by maximin Latin hypercube sampling [27], and each optimisation run was repeated 51 times with different initialisation. The same set of 51 initial observations were used for each of the mean functions to enable statistical comparisons. The hyperparameters θ of the GP were optimised by maximising the marginal log likelihood (8) with L-BFGS-B [8] using 10 restarts. Following common practise, maximisation of the acquisition functions was carried out via multi-start optimisation; details of the full procedure can be found in [3]. The trade-off between exploitation and exploration in UCB, β_t , is set to Theorem 1 in [39], which increases logarithmically with the number of function evaluations, with $\sqrt{\beta_t}$ approximately in the range [3, 6]. The Bayesian optimisation pipeline and mean functions were implemented with BoTorch [3] and code is available online² to recreate all experiments, as well as the LHS initialisations used and full optimisation runs.

Optimisation quality is measured with simple regret R_t , which is the difference between the true minimum value $f(\mathbf{x}^*)$ and the best value found so far after t evaluations:

$$R_t = |f(\mathbf{x}^*) - \min\{f_1, f_2, \dots, f_t\}|. \quad (12)$$

4.1 Synthetic Experiments

The mean functions were evaluated on the ten popular synthetic benchmark functions listed in Table 1 with a budget of 200 function evaluations that included the initial $2d$ LHS samples. These functions were selected due to their different dimensionality and landscape properties, such the presence of multiple local or global minima (Ackley, Eggholder, Hartmann6, GoldsteinPrice, StyblinskiTang, Shekel) deep, valley-like regions (Branin, Rosenbrock, SixHumpCamel), and steep ridges and drops (Michalewicz).

²<http://www.github.com/georgedeath/boeans>

Name	d	Name	d
Branin	2	Ackley	5
Eggholder	2	Hartmann6	6
GoldsteinPrice	2	Michalewicz	10
SixHumpCamel	2	Rosenbrock	10
Shekel	4	StyblinskiTang	10

Table 1: Synthetic functions used and their dimensionality d . Formulae for all functions can be found at <http://www.sfu.ca/~ssurjano/optimization.html>.

Table 2 shows the median regret over the 51 repeated experiments, together with the median absolute deviation from the median (MAD) for the mean functions using the EI acquisition function. Due to space constraints, the corresponding table for UCB is included in the supplementary material. The method with the lowest (best) median regret on each function is highlighted in dark grey, and those highlighted in light grey are statistically equivalent to the best method according to a one-sided paired Wilcoxon signed-rank test [24] with Holm-Bonferroni correction [18] ($p \geq 0.05$).

The convergence of the various mean functions on 8 illustrative test problems are shown using the EI (Figure 2) and UCB (Figure 3) acquisition functions. Convergence plots for the Branin and GoldsteinPrice test problems were visually similar to Eggholder and SixHumpCamel respectively; they are available in the supplementary material. As one might expect, because points are naturally less distant from one another, the choice of mean function has less impact in 2 dimensions. Although, interestingly, optimisation runs with the UCB algorithm in $d = 2$ achieve lower regret with the constant mean functions compared to the others evaluated.

Perhaps surprisingly, the non-constant mean functions, *Linear*, *Quadratic*, *RandomForest* and *RBF*, appear to offer no advantage over the constant mean functions despite their ability to model the large scale optimisation landscape. The *Quadratic* model, in two dimensions where there are only three parameters to be fitted, appears to be well suited to the SixHumpCamel function which is roughly bowl-shaped (albeit with quartic terms); however, this appears to be an exceptional case.

In higher dimensions with the EI acquisition function, using the worst observation value as the constant mean function (*Max*) consistently provides the lowest regret on the test functions evaluated. This is consistent with recent work [12, 35] showing that being more exploitative in higher dimensions is preferable to most other strategies. However, for the UCB acquisition function this is not the case and no mean function is consistently best. We suspect that this is because the value of β_t is so large that the UCB function (3) is always dominated by the exploratory term ($\sqrt{\beta_t} \sigma(\mathbf{x})$) so that the mean function has relatively little influence. This is in contrast to EI, which has been shown [12] to be far more exploitative than UCB.

The standard choice of using a constant mean function equal to \bar{f} the arithmetic mean of the observations (*Arithmetic*) is, in higher dimensions ($d \geq 5$), only statistically equivalent to the best-performing method on one of the five test functions for both EI and UCB. This result calls into question the efficacy of the common

practise of using the \bar{f} constant mean function in all Bayesian optimisation tasks. Based on these results we suggest that an increase in performance may be obtained by using the *Max* mean function with EI. Although there does not appear to be such a clear-cut answer as to which mean function should be used in conjunction with the UCB acquisition function, we posit that this is less important because, based on these optimisation results, one would prefer the performance of EI over UCB in general.

4.2 Active Learning for Robot Pushing

Like [11, 12, 21, 42] we optimise the control parameters for two active learning robot pushing problems [41]; see [12] for a diagrammatic outline of the problems. In the $d = 4$ PUSH4 problem, a robot should push an object towards an unknown target location and is constrained such that it can only travel in the initial direction of the object. Once the robot has finished pushing, it receives feedback in the form of the object-target distance. The robot is parametrised by its initial location, the orientation of its pushing hand and how long it pushes for. This can therefore be cast as a minimisation problem in which the four parameter values are optimised with respect to the object’s final distance from the target. The object’s initial location is fixed to the centre of the problem domain [42] and the target location is changed for each of the 51 optimisation runs, with these kept the same across mean functions. Thus, the optimisation performance is considered over problem instances rather than initialisations of a single instance.

The second problem, PUSH8, two robots push their respective objects towards two unknown targets, with their movements constrained so that they always travel in the direction of their object’s initial location. The $d = 8$ parameters controlling the robots can be optimised to minimise the summed final object-target distances. Like PUSH4, initial object locations were fixed for problem instances and the targets’ locations were chosen randomly, with a constraint enforcing that both objects could cover the targets without overlapping. This means, however, that in some problem instances it may not be possible for both robots to push their objects to their respective targets because they will block each other. Thus, for PUSH8 we report the final summed object-distances rather than the regret due to the global optimum not being known.

Figure 4 shows the convergence plots using the various mean functions with the EI and UCB acquisition functions. Tabulated results are available in the supplementary material. In the four-dimensional PUSH4 problem, one of the worst-performing mean functions on the synthetic functions, *RandomForest*, had substantially lower regret than the other mean functions using UCB on both problems and for EI on PUSH4. However, in the eight-dimensional PUSH8, all mean functions were statistically equivalent when using EI, apart from *Min*, *Linear* and *RBF*, which were worse. However, when using UCB, the *RandomForest* mean function was statistically better than all other mean functions, and it achieved results comparable to using EI.

It might be suspected that the superior ability of the Random Forest (and RBF on some problems) to represent the inherently difficult landscape features of these problems would account for the better performance of *RandomForest*. The landscape for these problems has sharp changes (high gradients) in the function, e.g. when

Table 2: Mean function performance using the EI acquisition function. Median regret (column left) and median absolute deviation from the median (MAD, column right) after 200 function evaluations across the 51 runs. The method with the lowest median performance is shown in dark grey, with those statistically equivalent shown in light grey.

Mean function	Branin (2)		Eggholder (2)		GoldsteinPrice (2)		SixHumpCamel (2)		Shekel (4)	
	Median	MAD	Median	MAD	Median	MAD	Median	MAD	Median	MAD
Arithmetic	1.35×10^{-5}	1.82×10^{-5}	1.58	1.93	4.18×10^{-2}	5.32×10^{-2}	2.51×10^{-5}	2.58×10^{-5}	8.13×10^{-2}	1.19×10^{-1}
Median	9.35×10^{-6}	1.17×10^{-5}	3.02	2.67	5.03×10^{-2}	5.59×10^{-2}	1.40×10^{-5}	1.49×10^{-5}	1.54×10^{-1}	2.24×10^{-1}
Min	1.18×10^{-5}	1.31×10^{-5}	2.82	3.13	6.25×10^{-2}	8.03×10^{-2}	2.25×10^{-5}	2.29×10^{-5}	7.02	9.75×10^{-1}
Max	7.21×10^{-6}	8.81×10^{-6}	2.69	2.48	6.87×10^{-2}	7.40×10^{-2}	1.52×10^{-5}	1.84×10^{-5}	7.16×10^{-2}	1.05×10^{-1}
Linear	5.13×10^{-6}	5.58×10^{-6}	2.82	2.85	1.05×10^{-1}	1.19×10^{-1}	7.98×10^{-6}	8.14×10^{-6}	6.47	1.57
Quadratic	1.05×10^{-5}	1.09×10^{-5}	3.59	4.03	5.55×10^{-2}	6.03×10^{-2}	6.27×10^{-6}	6.52×10^{-6}	6.47	1.30
RandomForest	5.35×10^{-4}	4.86×10^{-4}	3.93	4.22	2.41	2.14	2.96×10^{-4}	3.56×10^{-4}	2.84	2.76
RBF	1.36×10^{-4}	1.07×10^{-4}	3.27	3.45	1.76	2.39	3.76×10^{-5}	4.63×10^{-5}	7.95	1.05

Mean function	Ackley (5)		Hartmann6 (6)		Michalewicz (10)		Rosenbrock (10)		StyblinskiTang (10)	
	Median	MAD	Median	MAD	Median	MAD	Median	MAD	Median	MAD
Arithmetic	4.27	6.06	4.00×10^{-3}	5.46×10^{-3}	7.22×10^{-2}	1.03×10^{-1}	8.38×10^2	3.27×10^2	6.47×10^1	2.58×10^1
Median	2.10	2.06	8.31×10^{-4}	1.02×10^{-3}	7.88×10^{-2}	1.12×10^{-1}	7.14×10^2	2.78×10^2	6.72×10^1	2.49×10^1
Min	4.64	9.59×10^{-1}	3.27×10^{-3}	3.72×10^{-3}	1.39	7.49×10^{-1}	7.00×10^2	2.21×10^2	8.15×10^1	2.78×10^1
Max	1.66	1.23	7.47×10^{-4}	9.88×10^{-4}	2.75×10^{-2}	3.72×10^{-2}	6.95×10^2	3.64×10^2	2.84×10^1	2.08×10^1
Linear	1.65×10^1	2.42	1.21×10^{-2}	1.32×10^{-2}	1.30	8.55×10^{-1}	1.93×10^3	1.02×10^3	1.10×10^2	2.99×10^1
Quadratic	9.83	5.81	9.95×10^{-3}	9.63×10^{-3}	1.03	6.84×10^{-1}	1.81×10^3	8.90×10^2	8.58×10^1	4.14×10^1
RandomForest	5.16	7.70×10^{-1}	8.12×10^{-2}	5.63×10^{-2}	1.25×10^{-1}	1.43×10^{-1}	4.21×10^3	2.29×10^3	7.27×10^1	1.78×10^1
RBF	7.90	1.94	2.75×10^{-1}	1.55×10^{-1}	9.05×10^{-1}	5.57×10^{-1}	2.73×10^3	1.32×10^3	1.17×10^2	2.86×10^1

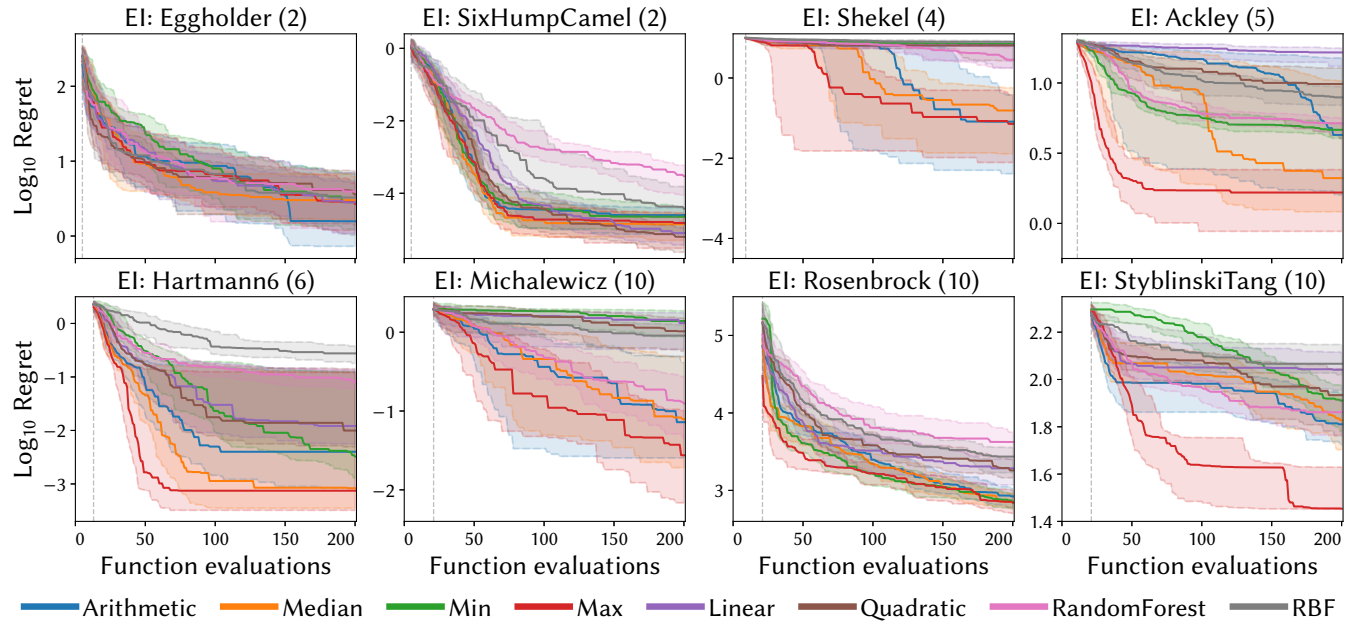


Figure 2: Illustrative convergence plots for eight benchmark problems using the EI acquisition function. Each plot shows the median regret, with shading representing the interquartile range across the 51 runs and the dashed vertical line indicating the end of the initial LHS phase.

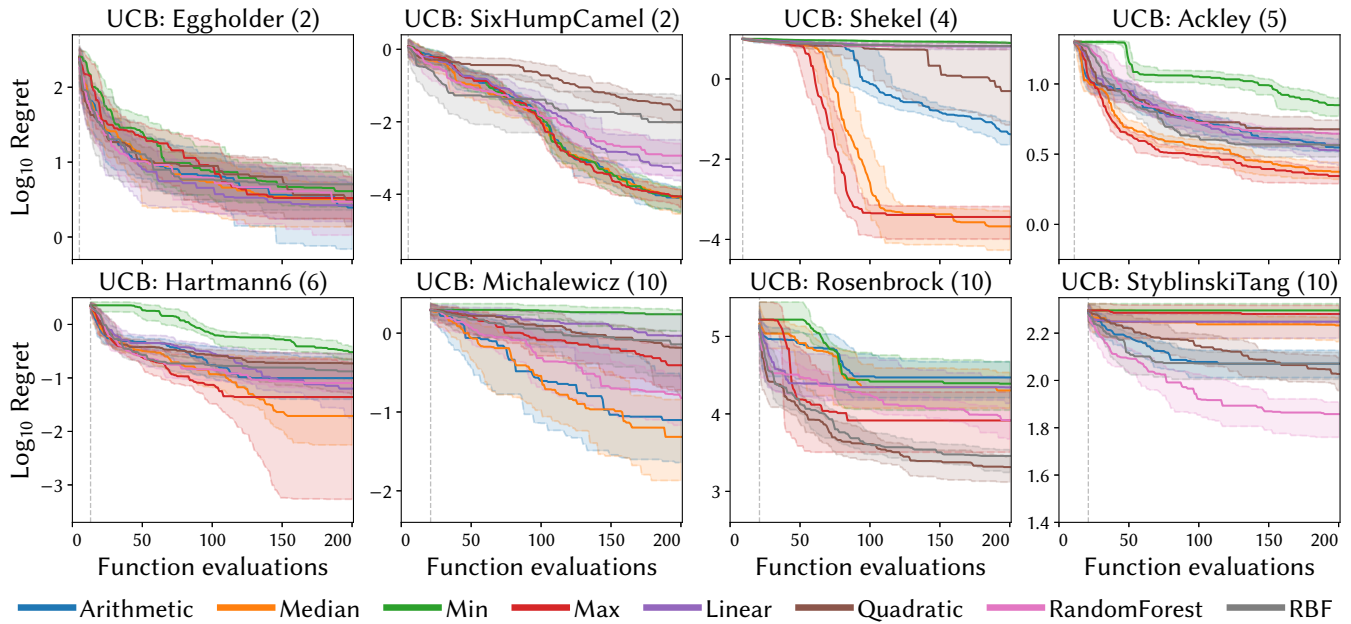


Figure 3: Illustrative convergence plots for eight benchmark problems using the UCB acquisition function. Each plot shows the median regret, with shading representing the interquartile range across the 51 runs and the dashed vertical line indicating the end of the initial LHS phase.

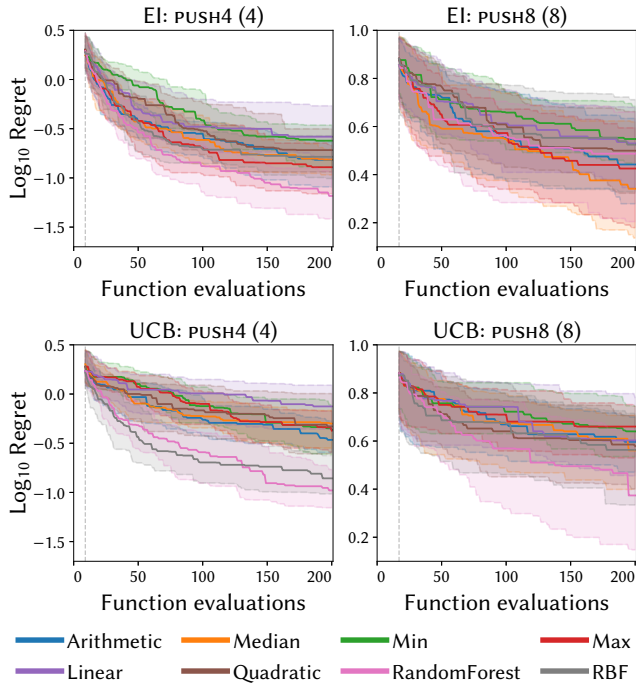


Figure 4: Convergence plots for the robot pushing problem using EI and UCB. Each plot shows the median regret, with shading representing the interquartile range of the 51 runs.

a change of the robot’s starting location results in the object no longer being pushed towards the target, as well as plateaux where changes in certain parameter values have little effect, e.g. if the amount of pushing time results in the robot not reaching the object. However, we investigated the mean prediction error of each of the combined mean plus Gaussian process models trained on the first 100 expensively evaluated locations by calculating the normalised root mean squared prediction error at 1000 locations (chosen by Latin Hypercube Sampling). As shown in the supplementary material, this indicates that, in fact, the RF model has a comparatively poor prediction error. By contrast, the RBF mean function yields the most accurate model of the overall landscape, but it only shows better performance for PUSH4 using UCB. These prediction errors were evaluated over the entire domain and, therefore, it is possible that the RF mean function is sufficiently superior in the vicinity of the optimum to allow the more rapid convergence seen here.

Interestingly, the performance of the *Max* mean function with EI on the synthetic test problems is not reflected on these two more real-world problems. However, both the *Arithmetic* and *Max* mean functions are statistically equivalent on both PUSH4 and PUSH8, with *Max* having lower median regret and MAD than *Arithmetic*. Nonetheless, it remains unclear why the RF mean function gives best performance in three of these four cases.

4.3 Pipe Shape Optimisation

Lastly, we evaluate the mean functions on a real-world computational fluid dynamics (CFD) optimisation problem. The goal of the PitzDaily CFD problem [9] is to minimise the pressure loss between a pipe’s entrance (inflow) and exit (outflow) by optimising the shape

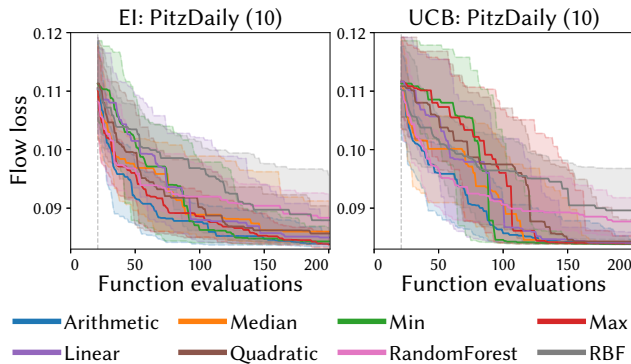


Figure 5: Convergence plots for the PitzDaily test problem using EI and UCB. Each plot shows the median regret, with shading representing the interquartile range of the 51 runs.

of the pipe’s lower wall. The loss is evaluated by generating a CFD mesh and simulating the two-dimensional flow using OpenFOAM [20], with each function evaluation taking between 60 and 90 seconds. The decision variables in the problem are the control points of a Catmull–Clark subdivision curve that represents the lower wall’s shape; see [9] for a pictorial representation of these. In this work we use 5 control points, resulting in a 10-dimensional decision vector. The control points are constrained to lie in a polygon, rather than a hypercube for all previous problems, and, therefore, we draw initial samples uniformly from within the constrained region rather than using LHS. Similarly, we use CMA-ES [16] to optimise the acquisition functions and penalise locations that violate the constraints.

Convergence plots of the flow loss for the mean functions with EI and UCB are shown in Figure 5. The *Arithmetic*, *Min* and *Max* constant mean functions, when using EI, are all statistically equivalent and the best-performing. It is interesting to note the contrasting performance between the *RandomForest* mean function on this and the robot pushing tasks.

As shown in Figure 5, using the UCB acquisition function leads to the constant mean and *Linear* mean functions all having a median flow loss within 10^{-4} of one another, with their inter-quartile ranges rapidly decreasing. This effect can also be seen towards the end of the optimisation runs with EI. Inspection of solutions (control points) with a flow loss ≈ 0.084 revealed that they all had distinct values but that they led to very similar sub-division curves. This implies that they all represented essentially the same inner wall shape and thus indicate the presence of either one large, valley-like global optimum or many, global optima. We suggest that this may be the actual minimum flow loss achievable for this problem. All mean functions, in combination with both EI and UCB, were able to successfully discover solutions that led to a flow loss of less than 0.0903 found by a local, gradient-based method in [30] that used approximately 500 function evaluations. This highlights the strength of Bayesian optimisation in general because the convergence rates shown in Figure 5 are far more rapid for the majority of mean functions and realise better solutions than the local, adjoint method.

5 CONCLUSION

We have investigated the effect of using different prior mean functions in the Gaussian process model during Bayesian optimisation when using the expected improvement and upper confidence bound acquisition functions. This was assessed by performing BO on ten synthetic functions and two real-world problems. The constant mean function *Max*, which uses a constant value of the worst-seen expensive function evaluation thus far, was found to consistently out-perform the other mean functions across the synthetic functions in higher dimensions, and was statistically equivalent to the best performing mean function on nine out of ten functions. We suggest that this is because this mean function tends to promote exploitation which can lead to rapid convergence in higher dimensions [12, 35] because exploration is implicitly provided through the necessarily inaccurate surrogate modelling. However, on the two, real-world problems this trend did not continue, but its performance was still statistically equivalent to the commonly-used mean equal to the arithmetic mean of the observations. For this reason we recommend using the *Max* mean function in conjunction with expected improvement for, at worst, the same performance as a zero mean and generally improved performance in higher dimensions.

Interestingly, the lack of consistency between mean function performance on the synthetic and real-world problems may indicate a larger issue in BO, namely that synthetic benchmarks do not always contain the same types of functional landscapes as real-world problems. In future work we would like to characterise a function’s landscape during the optimisation procedure and adaptively select the best-performing components of the BO pipeline, e.g. mean function, kernel, and acquisition function, to suit the problem structure.

This work focused on learning a mean function independent of the training of the GP. In further work we would like to jointly learn the parameters of the mean function, i.e. the weights in (9), alongside the hyperparameters of the GP itself. The efficacy of the BO approach clearly depends crucially on the ability of the surrogate model to accurately predict the function’s value in unvisited locations. We therefore look forward to evaluating a fully-Bayesian approach that marginalises over the mean function parameters and kernel hyperparameters. Although the Monte Carlo sampling required to evaluate the resulting acquisition functions may be substantial, an important area of investigation is whether fully-Bayesian models can significantly improve the convergence of Bayesian Optimisation.

ACKNOWLEDGMENTS

This work was supported by Innovate UK [grant number 104400].

REFERENCES

- [1] Erdem Acar. 2013. Effects of the correlation model, the trend model, and the number of training points on the accuracy of Kriging metamodels. *Expert Systems* 30, 5 (2013), 418–428.
- [2] The GPyOpt authors. 2016. GPyOpt: A Bayesian Optimization framework in python. <http://github.com/SheffieldML/GPyOpt>.
- [3] Maximilian Balandat, Brian Karrer, Daniel R. Jiang, Samuel Daulton, Benjamin Letham, Andrew Gordon Wilson, and Eytan Bakshy. 2019. BoTorch: Programmable Bayesian Optimization in PyTorch. arXiv:1910.06403
- [4] Christopher M. Bishop. 2006. *Pattern Recognition and Machine Learning*. Springer, Berlin, Heidelberg.

- [5] B. J. N. Blight and L. Ott. 1975. A Bayesian approach to model inadequacy for polynomial regression. *Biometrika* 62, 1 (1975), 79–88.
- [6] Leo Breiman. 2001. Random Forests. *Machine Learning* 45, 1 (2001), 5– 32.
- [7] Eric Brochu, Vlad M Cora, and Nando De Freitas. 2010. A tutorial on Bayesian optimization of expensive cost functions, with application to active user modeling and hierarchical reinforcement learning. arXiv:1012.2599
- [8] Richard H Byrd, Peihuang Lu, Jorge Nocedal, and Ciyou Zhu. 1995. A limited memory algorithm for bound constrained optimization. *SIAM Journal on Scientific Computing* 16, 5 (1995), 1190–1208.
- [9] Steven J. Daniels, Alma A. M. Rahat, Richard M. Everson, Gavin R. Tabor, and Jonathan E. Fieldsend. 2018. A Suite of Computationally Expensive Shape Optimization Problems Using Computational Fluid Dynamics. In *Parallel Problem Solving from Nature – PPSN XV*. Springer, 296–307.
- [10] Alex Davies and Zoubin Ghahramani. 2014. The Random Forest Kernel and other kernels for big data from random partitions. arXiv:1402.4293
- [11] George De Ath, Richard M. Everson, Jonathan E. Fieldsend, and Alma A. M. Rahat. 2020. ϵ -shotgun: ϵ -greedy Batch Bayesian Optimisation. In *Proceedings of the Genetic and Evolutionary Computation Conference*. Association for Computing Machinery.
- [12] George De Ath, Richard M. Everson, Alma A. M. Rahat, and Jonathan E. Fieldsend. 2019. Greed is Good: Exploration and Exploitation Trade-offs in Bayesian Optimisation. arXiv:1911.12809
- [13] Vincent Fortuin, Heiko Strathmann, and Gunnar R dtsch. 2019. Meta-Learning Mean Functions for Gaussian Processes. arXiv:1901.08098
- [14] Peter I Frazier. 2018. A tutorial on Bayesian optimization. arXiv:1807.02811
- [15] Pierre Geurts, Damien Ernst, and Louis Wehenkel. 2006. Extremely randomized trees. *Machine Learning* 63, 1 (2006), 3–42.
- [16] Nikolaus Hansen. 2009. Benchmarking a BI-population CMA-ES on the BBOB-2009 function testbed. In *Proceedings of the 11th Annual Conference Companion on Genetic and Evolutionary Computation Conference: Late Breaking Papers*. ACM, 2389–2396.
- [17] Jos  Miguel Hern ndez-Lobato, Matthew W Hoffman, and Zoubin Ghahramani. 2014. Predictive Entropy Search for Efficient Global Optimization of Black-box Functions. In *Advances in Neural Information Processing Systems*. Curran Associates, Inc., 918–926.
- [18] Sture Holm. 1979. A simple sequentially rejective multiple test procedure. *Scandinavian Journal of Statistics* 6, 2 (1979), 65–70.
- [19] Tomoharu Iwata and Zoubin Ghahramani. 2017. Improving Output Uncertainty Estimation and Generalization in Deep Learning via Neural Network Gaussian Processes. arXiv:1707.05922
- [20] Hrvoje Jasak, Aleksandar Jemcov, and  eljko Tukovi . 2007. OpenFOAM: A C++ Library for Complex Physics Simulations. In *International Workshop on Coupled Methods in Numerical Dynamics*. 1–20.
- [21] Shali Jiang, Henry Chai, Javier Gonz lez, and Roman Garnett. 2019. Efficient nonmyopic Bayesian optimization and quadrature. arXiv:1909.04568
- [22] Donald R. Jones, Matthias Schonlau, and William J. Welch. 1998. Efficient Global Optimization of Expensive Black-Box Functions. *Journal of Global Optimization* 13, 4 (1998), 455–492.
- [23] Marc C. Kennedy and Anthony O’Hagan. 2001. Bayesian calibration of computer models. *Journal of the Royal Statistical Society: Series B (Statistical Methodology)* 63, 3 (2001), 425–464.
- [24] Joshua D. Knowles, Lothar Thiele, and Eckart Zitzler. 2006. *A Tutorial on the Performance Assessment of Stochastic Multiobjective Optimizers*. Technical Report TIK214. Computer Engineering and Networks Laboratory, ETH Zurich, Zurich, Switzerland.
- [25] Harold J. Kushner. 1964. A new method of locating the maximum point of an arbitrary multipeak curve in the presence of noise. *Journal Basic Engineering* 86, 1 (1964), 97–106.
- [26] Marius Lindauer, Matthias Feurer, Katharina Eggensperger, Andr  Biedenkapp, and Frank Hutter. 2019. Towards Assessing the Impact of Bayesian Optimization’s Own Hyperparameters. In *IJCAI 2019 DSO Workshop*.
- [27] Micheal D. McKay, Richard J. Beckman, and William J. Conover. 2000. A comparison of three methods for selecting values of input variables in the analysis of output from a computer code. *Technometrics* 42, 1 (2000), 55–61.
- [28] Jonas Mockus, Vytautas Tiesis, and Antanas Zilinskas. 1978. The application of Bayesian methods for seeking the extremum. *Towards Global Optimization* 2, 1 (1978), 117–129.
- [29] Tanmoy Mukhopadhyay, S Chakraborty, S Dey, S Adhikari, and R Chowdhury. 2017. A critical assessment of Kriging model variants for high-fidelity uncertainty quantification in dynamics of composite shells. *Archives of Computational Methods in Engineering* 24, 3 (2017), 495–518.
- [30] Ulf Nilsson, Daniel Lindblad, and Olivier Petit. 2014. *Description of adjointShapeOptimizationFoam and how to implement new objective functions*. Technical Report. Chalmers University of Technology, Gothenburg, Sweden.
- [31] Mark J. L. Orr. 1996. *Introduction to radial basis function networks*. Technical Report. University of Edinburgh.
- [32] Pramudita Satria Palar and Koji Shimoyama. 2019. Efficient global optimization with ensemble and selection of kernel functions for engineering design. *Structural and Multidisciplinary Optimization* 59, 1 (2019), 93–116.
- [33] Pramudita S. Palar, Lavi R. Zuhail, Tinkle Chugh, and Alma Rahat. 2020. On the Impact of Covariance Functions in Multi-Objective Bayesian Optimization for Engineering Design. In *AIAA Scitech 2020 Forum*. American Institute of Aeronautics and Astronautics.
- [34] Carl Edward Rasmussen and Christopher K. I. Williams. 2006. *Gaussian processes for machine learning*. The MIT Press, Boston, MA.
- [35] Frederik Rehbach, Martin Zaefferer, Boris Naujoks, and Thomas Bartz-Beielstein. 2020. Expected Improvement versus Predicted Value in Surrogate-Based Optimization. arXiv:2001.02957
- [36] Erwan Scornet. 2016. Random Forests and Kernel Methods. *IEEE Transactions on Information Theory* 62, 3 (2016), 1485–1500.
- [37] Bobak Shahriari, Kevin Swersky, Ziyu Wang, Ryan P. Adams, and Nando de Freitas. 2016. Taking the human out of the loop: A review of Bayesian optimization. *Proc. IEEE* 104, 1 (2016), 148–175.
- [38] Jasper Snoek, Hugo Larochelle, and Ryan P Adams. 2012. Practical Bayesian optimization of machine learning algorithms. In *Advances in Neural Information Processing Systems*. Curran Associates, Inc., 2951–2959.
- [39] Niranjan Srinivas, Andreas Krause, Sham Kakade, and Matthias Seeger. 2010. Gaussian process optimization in the bandit setting: no regret and experimental design. In *Proceedings of the 27th International Conference on Machine Learning*. Omnipress, 1015–1022.
- [40] Michael L Stein. 2012. *Interpolation of spatial data: some theory for kriging*. Springer Science & Business Media.
- [41] Zi Wang, Caelan Reed Garrett, Leslie Pack Kaelbling, and Tom s Lozano-P rez. 2018. Active Model Learning and Diverse Action Sampling for Task and Motion Planning. In *Proceedings of the International Conference on Intelligent Robots and Systems*. IEEE, 4107–4114.
- [42] Zi Wang and Stefanie Jegelka. 2017. Max-value entropy search for efficient Bayesian optimization. In *Proceedings of the 34th International Conference on Machine Learning*. PMLR, 3627–3635.
- [43] Daniel Williamson, Adam T Blaker, Charlotte Hampton, and James Salter. 2015. Identifying and removing structural biases in climate models with history matching. *Climate dynamics* 45, 5 (2015), 1299–1324.
- [44] David H. Wolpert and William G. Macready. 1997. No free lunch theorems for optimization. *IEEE Transactions on Evolutionary Computation* 1, 1 (1997), 67–82.

What do you Mean?

The Role of the Mean Function in Bayesian Optimisation

Supplementary Material

GEORGE DE ATH, University of Exeter, United Kingdom
 JONATHAN E. FIELDSEND, University of Exeter, United Kingdom
 RICHARD M. EVERSON, University of Exeter, United Kingdom

ACM Reference Format:

George De Ath, Jonathan E. Fieldsend, and Richard M. Everson. 2020. What do you Mean? The Role of the Mean Function in Bayesian Optimisation: Supplementary Material. In *Genetic and Evolutionary Computation Conference Companion (GECCO '20 Companion)*, July 8–12, 2020, Cancun, Mexico. ACM, New York, NY, USA, 4 pages. <https://doi.org/10.1145/3377929.3398118>

A ADDITIONAL RESULTS

In this section we show convergence plots for the Branin and GoldsteinPrice synthetic test functions for both the EI and UCB acquisition functions, as well as the results tables for UCB on the synthetic functions, and EI and UCB on the three real-world problems.

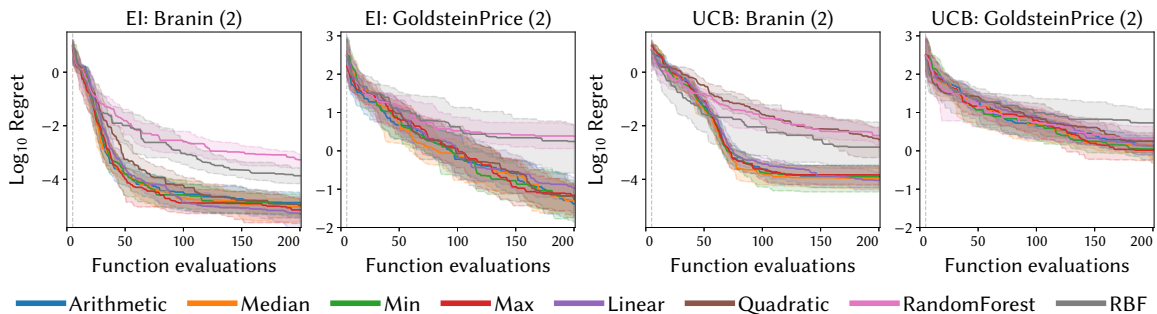


Fig. 1. Convergence plots for the Branin and GoldsteinPrice test problem using EI (*left*) and UCB (*right*). Each plot shows the median regret, with shading representing the interquartile range across the 51 runs.

GECCO '20 Companion, July 8–12, 2020, Cancun, Mexico

© 2020 Copyright held by the owner/author(s). Publication rights licensed to ACM.

This is the author's version of the work. It is posted here for your personal use. Not for redistribution. The definitive Version of Record was published in *Genetic and Evolutionary Computation Conference Companion (GECCO '20 Companion)*, July 8–12, 2020, Cancun, Mexico, <https://doi.org/10.1145/3377929.3398118>.

Table 1. Mean function performance using the UCB acquisition function. Median regret (*column left*) and median absolute deviation from the median (MAD, *column right*) after 200 function evaluations across the 51 runs. The method with the lowest median performance is shown in dark grey, with those statistically equivalent shown in light grey.

Mean function	Branin (2)		Eggholder (2)		GoldsteinPrice (2)		SixHumpCamel (2)		Shekel (4)	
	Median	MAD	Median	MAD	Median	MAD	Median	MAD	Median	MAD
Arithmetic	1.27×10^{-4}	1.47×10^{-4}	2.47	2.77	1.37	1.24	7.94×10^{-5}	7.12×10^{-5}	4.20×10^{-2}	3.38×10^{-2}
Median	1.11×10^{-4}	1.44×10^{-4}	3.21	2.76	1.21	9.88×10^{-1}	7.44×10^{-5}	7.44×10^{-5}	2.11×10^{-4}	2.89×10^{-4}
Min	1.27×10^{-4}	1.57×10^{-4}	4.09	3.09	1.12	9.27×10^{-1}	8.57×10^{-5}	9.33×10^{-5}	7.88	6.60×10^{-1}
Max	1.46×10^{-4}	1.55×10^{-4}	3.31	3.01	1.04	1.09	8.75×10^{-5}	7.29×10^{-5}	3.63×10^{-4}	4.03×10^{-4}
Linear	9.20×10^{-5}	8.31×10^{-5}	2.66	2.34	1.36	8.95×10^{-1}	4.53×10^{-4}	5.47×10^{-4}	6.47	7.89×10^{-2}
Quadratic	3.05×10^{-3}	4.36×10^{-3}	3.08	4.15	1.78	1.59	2.15×10^{-2}	2.01×10^{-2}	4.98×10^{-1}	7.31×10^{-1}
RandomForest	4.30×10^{-3}	4.55×10^{-3}	2.96	3.30	2.18	1.49	1.16×10^{-3}	1.40×10^{-3}	6.61	1.76
RBF	1.59×10^{-3}	2.21×10^{-3}	5.05	4.05	5.36	6.16	9.78×10^{-3}	1.43×10^{-2}	6.64	1.60

Mean function	Ackley (5)		Hartmann6 (6)		Michalewicz (10)		Rosenbrock (10)		StyblinskiTang (10)	
	Median	MAD	Median	MAD	Median	MAD	Median	MAD	Median	MAD
Arithmetic	3.53	6.53×10^{-1}	9.93×10^{-2}	1.22×10^{-1}	7.90×10^{-2}	9.42×10^{-2}	2.95×10^4	2.36×10^4	1.18×10^2	2.40×10^1
Median	2.37	5.60×10^{-1}	1.94×10^{-2}	2.70×10^{-2}	4.84×10^{-2}	5.89×10^{-2}	2.00×10^4	1.61×10^4	1.71×10^2	2.97×10^1
Min	7.06	1.49	3.03×10^{-1}	1.29×10^{-1}	1.74	6.51×10^{-1}	2.45×10^4	2.21×10^4	1.98×10^2	2.57×10^1
Max	2.21	4.51×10^{-1}	4.40×10^{-2}	6.48×10^{-2}	3.92×10^{-1}	3.59×10^{-1}	8.22×10^3	8.89×10^3	1.91×10^2	2.52×10^1
Linear	3.35	8.75×10^{-1}	6.31×10^{-2}	8.03×10^{-2}	9.27×10^{-1}	1.13	2.20×10^4	1.20×10^4	1.77×10^2	2.94×10^1
Quadratic	4.75	1.71	1.87×10^{-1}	1.84×10^{-1}	6.54×10^{-1}	5.72×10^{-1}	2.06×10^3	1.10×10^3	1.06×10^2	2.47×10^1
RandomForest	4.42	5.62×10^{-1}	8.03×10^{-2}	6.30×10^{-2}	1.51×10^{-1}	1.59×10^{-1}	8.27×10^3	4.96×10^3	7.21×10^1	1.75×10^1
RBF	3.67	1.05	1.33×10^{-1}	6.83×10^{-2}	7.21×10^{-1}	5.60×10^{-1}	2.87×10^3	1.18×10^3	1.18×10^2	2.12×10^1

Table 2. Mean function performance using the EI (*left table*) and UCB (*right table*) acquisition functions. Median regret (*column left*) and median absolute deviation from the median (MAD, *column right*) after 200 function evaluations across the 51 runs are shown in paired columns. The method with the lowest median performance is shown in dark grey, with those statistically equivalent in light grey.

Mean function	PUSH4 (4)		PUSH8 (8)		Mean function	PUSH4 (4)		PUSH8 (8)	
	Median	MAD	Median	MAD		Median	MAD	Median	MAD
Arithmetic	1.53×10^{-1}	1.16×10^{-1}	2.77	1.93	Arithmetic	3.42×10^{-1}	2.18×10^{-1}	3.95	1.57
Median	1.54×10^{-1}	6.53×10^{-2}	2.19	1.58	Median	5.01×10^{-1}	3.06×10^{-1}	3.64	2.05
Min	2.39×10^{-1}	1.60×10^{-1}	3.53	1.44	Min	4.36×10^{-1}	3.69×10^{-1}	4.37	1.72
Max	1.28×10^{-1}	9.75×10^{-2}	2.66	1.83	Max	4.25×10^{-1}	3.20×10^{-1}	4.57	1.74
Linear	2.62×10^{-1}	2.10×10^{-1}	3.39	2.05	Linear	7.48×10^{-1}	5.47×10^{-1}	4.00	2.70
Quadratic	1.92×10^{-1}	1.28×10^{-1}	3.16	1.83	Quadratic	4.69×10^{-1}	4.37×10^{-1}	3.79	1.94
RandomForest	6.56×10^{-2}	5.71×10^{-2}	3.07	2.24	RandomForest	1.05×10^{-1}	6.92×10^{-2}	2.36	2.11
RBF	1.64×10^{-1}	1.19×10^{-1}	3.35	2.29	RBF	1.39×10^{-1}	9.29×10^{-2}	3.66	2.43

Table 3. Mean function performance using the EI (*left table*) and UCB (*right table*) acquisition functions. Median regret (*column left*) and median absolute deviation from the median (MAD, *column right*) after 200 function evaluations across the 51 runs are shown in paired columns. The method with the lowest median performance is shown in dark grey, with those statistically equivalent in light grey.

Mean function	PitzDaily (10)		Mean function	PitzDaily (10)	
	Median	MAD		Median	MAD
Arithmetic	8.39 × 10 ⁻²	1.12 × 10 ⁻³	Arithmetic	8.41 × 10 ⁻²	3.92 × 10 ⁻⁴
Median	8.60 × 10 ⁻²	3.23 × 10 ⁻³	Median	8.40 × 10 ⁻²	1.96 × 10 ⁻⁴
Min	8.43 × 10 ⁻²	1.39 × 10 ⁻³	Min	8.39 × 10 ⁻²	2.01 × 10 ⁻⁴
Max	8.38 × 10 ⁻²	1.38 × 10 ⁻³	Max	8.40 × 10 ⁻²	3.07 × 10 ⁻⁴
Linear	8.50 × 10 ⁻²	2.24 × 10 ⁻³	Linear	8.41 × 10 ⁻²	3.98 × 10 ⁻⁴
Quadratic	8.57 × 10 ⁻²	3.07 × 10 ⁻³	Quadratic	8.43 × 10 ⁻²	9.23 × 10 ⁻⁴
RandomForest	8.84 × 10 ⁻²	6.38 × 10 ⁻³	RandomForest	8.77 × 10 ⁻²	4.69 × 10 ⁻³
RBF	8.79 × 10 ⁻²	6.23 × 10 ⁻³	RBF	8.96 × 10 ⁻²	8.23 × 10 ⁻³

B GP MODELLING ERROR USING DIFFERENT MEAN FUNCTIONS

In this section we present a short investigation into the modelling capability of the Gaussian process (GP) when combined with different mean functions. In order to quantify the modelling capability of a GP using a prior mean function on a test function $f : \mathbb{R}^d \mapsto \mathbb{R}$, we created GP models of f using training data taken from the optimisation runs, evaluated a set of $N = 1000$ test locations, and calculated the model’s normalised root mean squared error (NRMSE).

More precisely, for a given test problem f , a GP model using the mean function to be evaluated was created using the first 100 locations (including initial LHS samples) for each of the mean function’s 51 optimisation runs using the EI acquisition function. A set of $N = 1000$ test locations $X = \{\mathbf{x}_n\}_{n=1}^N$ were chosen via Latin hypercube sampling and the model’s prediction NRMSE between the true function values f_n and predicted values from the surrogate model \hat{f}_n were calculated for each of the 51 models. The NRMSE is defined as

$$\text{NRMSE} = \frac{\sqrt{\frac{1}{N} \sum_{n=1}^N (f_n - \hat{f}_n)^2}}{f_{\max} - f_{\min}}, \quad (1)$$

where f_{\max} and f_{\min} are the largest and smallest values of the test locations evaluated using the real function. The test locations X were paired across models corresponding to optimisation runs using the same training data so that a statistical comparison could be undertaken.

Table 4 shows the median NRMSE over the 51 GP models created using each mean function for the synthetic and robot pushing test problems. The method with the lowest median NRMSE on each function is highlighted in dark grey, and those highlighted in light grey are statistically equivalent to the best method according to a one-sided paired Wilcoxon signed-rank test with Holm-Bonferroni correction ($p \geq 0.05$). The RBF mean function provides the best (or equivalent to the best) modelling error for the evaluated test locations on 10 of the 12 evaluated functions. Interestingly, this does not correspond the same performance in Bayesian optimisation (recall Table 1 in the main paper). We suspect this is because the experiments are evaluating modelling of the entire function, whereas BO only requires the GP model to reflect the true function within the region that the minima reside.

Further work in quantifying the modelling error in BO could be carried out by only calculating the NRMSE within a small hypercube surrounding the global optimum. However, the size of the hypercube required to accurately calculate the modelling error of the important features for BO may vary between problems and therefore additional evaluations may be required of sets of test data sampled from hypercubes of different sizes.

	Arith	Med	Min	Max	Lin	Quad	RF	RBF
Branin	0.271	0.271	0.271	0.263	0.270	0.263	0.121	0.114
Eggholder	0.217	0.165	0.216	0.177	0.161	0.163	0.198	0.166
GoldsteinPrice	0.136	0.136	0.136	0.136	0.136	0.136	0.069	0.136
SixHumpCamel	0.232	0.231	0.231	0.223	0.215	0.216	0.142	0.228
Shekel	0.265	0.215	0.494	0.058	0.083	0.094	0.142	0.053
Ackley	0.663	0.716	0.316	0.899	0.107	0.378	0.334	0.117
Hartmann6	0.222	0.394	0.184	0.154	0.140	0.185	0.195	0.097
Michalewicz	0.271	0.311	0.417	0.316	0.205	0.193	0.360	0.190
Rosenbrock	0.362	0.368	0.371	0.270	0.257	0.151	0.355	0.157
StyblinskiTang	0.325	0.347	0.360	0.151	0.267	0.199	0.220	0.168
PUSH4	0.202	0.200	0.256	0.254	0.153	0.152	0.222	0.151
PUSH8	0.205	0.202	0.238	0.168	0.136	0.129	0.191	0.125

Table 4. Median NRMSE modelling prediction error taken over across 51 GP models using the the 8 evaluated mean functions on the ten synthetic and two robot pushing functions. The models with the lowest NRMSE are shown in dark grey, with those statistically equivalent to them shown in light grey.